Chromosome Research **13**: 135–144, 2005.

Different populations of RNA polymerase II in living mammalian cells

Miki Hieda[1,2], Henry Winstanley[3], Philip Maini[4], Francisco J. Iborra[1,5] & Peter R. Cook[1*]
[1]*Sir William Dunn School of Pathology, University of Oxford, South Parks Road, Oxford, OX1 3RE, UK; Tel: (+44/0)1865 275528; Fax: (+44/0) 14865 275515; E-mail: peter.cook@path.ox.ac.UK;* [2]*Current address: Department of Medical Biochemistry, Ehime University School of Medicine, Onsen-gun, Ehime 791–0295, Japan;* [3]*Life Sciences Interface DTC, University of Oxford, Peter Medawar Building, South Parks Road, Oxford, OX1 3SY, UK;* [4]*Centre for Mathematical Biology, Mathematical Institute, University of Oxford, 24–29 St Giles; Oxford, OX1 3LB, UK;* [5]*Current address: MRC Molecular Haematology Unit, Weatherall Institute of Molecular Medicine, John Radcliffe Hospital, Headington, Oxford, OX3 9DS, UK*
**Correspondence*

Received 23 November 2004. Received in revised form and accepted for publication by Herbert Macgregor 10 December 2004

Key words: DRB, FLIP, heat shock, photobleaching, RNA polymerase II

Abstract

RNA polymerase II is responsible for transcription of most eukaryotic genes, but, despite exhaustive analysis, little is known about how it transcribes natural templates *in vivo*. We studied polymerase dynamics in living Chinese hamster ovary cells using an established line that expresses the largest (catalytic) subunit of the polymerase (RPB1) tagged with the green fluorescent protein (GFP). Genetic complementation has shown this tagged polymerase to be fully functional. Fluorescence loss in photobleaching (FLIP) reveals the existence of at least three kinetic populations of tagged polymerase: a large rapidly-exchanging population, a small fraction resistant to 5,6-dichloro-1-β-D-ribofuranosylbenzimidazole (DRB) but sensitive to a different inhibitor of transcription (i.e. heat shock), and a third fraction sensitive to both inhibitors. Quantitative immunoblotting shows the largest fraction to be the inactive hypophosphorylated form of the polymerase (i.e. II_A). Results are consistent with the second (DRB-insensitive but heat-shock-sensitive) fraction being bound but not engaged, while the third (sensitive to both DRB and heat shock) is the elongating hyperphosphorylated form (i.e. II_O).

Introduction

RNA polymerase II transcribes most eukaryotic genes. Although systematic analysis has given us detailed information on how this enzyme with 12 conserved subunits initiates, elongates, and terminates on naked DNA templates *in vitro* (Lee & Young 2000, Woychik & Hampsey 2002, Shilatifard *et al.* 2003, Asturias 2004), little is yet known about how it transcribes natural templates *in vivo*. In order to study polymerase dynamics in living cells, we developed a cell line that expresses the largest (catalytic) subunit, RPB1, tagged with the green fluorescent protein (GFP). This autofluorescent protein is widely used to tag proteins so they can be localized easily (Tsien 1998). Application of techniques like FRAP (fluorescent recovery after photobleaching) and FLIP (fluorescence loss in photobleaching) then allows measurement of diffusion

coefficients, rates of exchange of the tagged protein between different cellular compartments, and the proportions of mobile and immobile fractions (Houtsmuller & Vermeulen 2001, Lippincott-Schwartz *et al.* 2001, Phair & Misteli 2001). For example, we and others have used these techniques to analyse the kinetics of RNA polymerases I and II *in vivo* (Becker *et al.* 2002, Dundr *et al.* 2002, Kimura *et al.* 2002).

Our cell line, C23, is derived from tsTM4, a temperature-sensitive mutant of the Chinese hamster ovary cell, CHO-K1. The mutation in tsTM4, which grows at 34°C but not at 39°C, has been mapped to RPB1 (Tsuji *et al.* 1990, Sugaya *et al.* 1997). The gene encoding wild-type human RPB1 was fused with another encoding GFP, and the construct expressed in tsTM4; the resulting GFP-tagged polymerase (GFP-pol) complemented the defect at the restrictive temperature (39°C), and so enabled normal growth (Sugaya *et al.* 2000). This indicates the tagged polymerase is functional at 39°C, as C23 cells depend on it for survival. However, C23 also contains the original temperature-sensitive (endogenous) enzyme that is used in conjunction with the GFP-pol at 34°C.

We went on to analyse the kinetics of the tagged polymerase in living C23 cells using both FRAP and FLIP (Kimura *et al.* 2002). We expected to find at least three fractions – a large pool of enzyme able to diffuse freely, a small fraction incorporated into the pre-initiation complex, and a third that was elongating and so temporarily immobilized on the template; the second fraction would probably be bound only temporarily, while the third would be bound for the time taken to make a transcript and it would be sensitive to inhibitors of transcriptional elongation. However, FRAP data could be fitted assuming there were only two kinetic fractions, with ~75% moving rapidly and ~25% being transiently immobile (association $t_{1/2}$ ~20 min). FLIP data were also consistent with the existence of two populations but were not analysed in detail, as the time between successive bleaches was too short to permit equilibration. Therefore, we concluded parsimoniously that the rapidly moving and transiently immobile populations were freely diffusing and engaged fractions, respectively. Identification of the transiently immobile fraction as the engaged one was supported by the finding that 5,6-dichloro-1-β-D-ribofuranosylbenzimidazole (DRB) – a transcriptional inhibitor that blocks the transition from initiation to elongation (Chodosh *et al.* 1989, Marshall & Price 1992, Yamaguchi *et al.* 1998) – reduced its size. Moreover, the half-life of the elongating fraction in wild-type cells – which could be measured by labelling with [^{3}H]uridine – was ~14 min and so roughly similar to that of the transiently immobile fraction.

We have now used FLIP to re-examine the kinetics of the GFP-pol in C23 cells. As before, we concentrate on changes occurring over the minutes required to complete a transcription cycle (i.e. including initiation, elongation, termination). [Determining whether GFP-pol diffuses as a core enzyme of ~500 kDa or larger complex of 1000–2000 kDa (Lee & Young, 2000) requires analysis over fractions of a second and the development of fluorescent standards of appropriate size.] Results are consistent with the existence of three (or more) populations: a large 'free' (rapidly-diffusing) one, a small fraction resistant to DRB but sensitive to a different inhibitor of transcription (i.e. heat shock), and the 'engaged' fraction sensitive to both inhibitors.

Materials and methods

Cell culture

C23 cells, a clonal derivative of tsTM4 cells expressing the largest subunit of polymerase II (RPB1) tagged with GFP under the control of the cytomegalovirus promoter (Sugaya *et al.* 2000), were grown at 39°C in Ham's F-12 medium (Invitrogen Ltd, Paisley, UK) plus 10% fetal calf serum.

FLIP

Cells were grown in glass-bottomed microwell dishes (Mat Tek, MA) for 40–48 h to 50% confluence. The standard FLIP experiment in Figure 1 was performed as described by Kimura *et al.* (2002) using a Radiance 2000 confocal microscope (488-nm-laser line; 25-mW argon laser at 4% power; 4× zoom; scan speed 600 lines/s; detection using LP500 filter and pinhole setting 4; image size 51.5 μm; BioRad Laboratories, Hemel Hampstead, UK) fitted on a TE300 microscope (Nikon UK Limited, Kingston upon Thames,

Surrey, UK) and a 60 × PlanApo objective (numerical aperture 1.4). Cells were imaged at 39°C on the microscope stage. A field with two cells was selected, imaged every ~0.43 s for 30 images, and the bottom half of one nucleus bleached with 100% laser power as the field was scanned every 0.43 s for another 130 s. The intensity of the unbleached half of the bleached nucleus was measured and normalized relative to the unbleached nucleus (Phair & Misteli 2000). Then, the relative intensity is given by:

$$\frac{[I_{(t)} - B_{(t)}]/[KI_{(t)} - B_{(t)}]}{[I_{(0)} - B_{(0)}]/[KI_{(0)} - B_{(0)}]}$$

where $I_{(t)}$ is the average intensity of the unbleached region of interest at time t, $I_{(0)}$ is the average prebleach intensity of the region of interest averaged over ~15 s, $KI_{(0)}$ and $KI_{(t)}$ are the average nuclear intensities of a neighbouring cell in the same field of view prior to bleaching and at time t, respectively, and $B_{(0)}$ and $B_{(t)}$ are the average background fluorescence outside cells in the same field prior to bleaching and at time t, respectively. The alternative procedure (Figure 2, curves 4, 5) used the laser at 2.5% power, 7× zoom, scan speed 500 lines/s, Kalman filter 7, pinhole setting 8, and data was collected every 15 s to allow complete equilibration of mobile proteins. As a result, each experiment involved repeats of 7 imaging/bleaching scans (over 3.58 s) and 11.42 s without illumination; the Kalman filter combined the 7 scans into one to provide images.

In some cases, 100 μmol/L 5,6-dichloro-1-β-D-ribofuranosylbenzimidazole (DRB) was added for 25 min before FLIP, so the total time in DRB until the last image was collected ranged from 25–57 min. The extent of transcriptional inhibition by the drug was monitored by immunofluorescence. Cells were grown in DRB for 25 or 60 min (the minimum and maximum exposures) and fixed; 2.5 mmol/L Br-U was added 10 min prior to fixation, and the resulting Br-RNA indirectly immunolabelled (below). Treatment with DRB for 25 and 60 min reduced nucleoplasmic labelling (measured as below using >100 cells) to 34 ± 12 and 16 ± 5% of untreated controls, respectively (not shown). As cells in the FLIP experiment in Figure 2 were analysed in this time interval, and as ~8% residual activity is due to polymerase III (Pombo *et al.* 1999), between 74 and 92% polymerase II would be inhibited.

In other cases, cells were heat shocked. The glass-bottomed microwell dish was surrounded in waxy film, immersed in a water bath for 15 min at 45°C, and incubated on the microscope stage at 45°C for up to another 20 min during FLIP (total time at 45°C was always <35 min). This treatment also inhibits most polymerase II activity; thus, in experiments like the one illustrated in Figure 1 C, the relative intensities of nucleoplasmic labelling (average of >30 nuclei) at the four times were 100, 51 ± 27, 12 ± 5, and 92 ± 48, respectively (not shown). As the maximum exposure of cells in the FLIP experiment in Figure 2 was 35 min, and as ~8% residual activity is due to polymerase III (Pombo *et al.* 1999), all but 4% polymerase II would then be inhibited. This value is close to the 92% maximal inhibition seen with DRB.

Data were analysed using kinetic models based on standard principles of chemical kinetics (Phair & Misteli 2001, Dundr *et al.* 2002) and 'BerkeleyMadonna' (http://www.berkeleymadonna.com) and 'MATLAB' software (http://www.mathworks.com). However, unconstrained optimization of parameters for various 3-population ordinary differential equation models yielded similar least-squares best fits (not shown), such that we were unable to discriminate conclusively between them. For example, in one model a 'free' population bound reversibly, and some of the resulting 'bound' fraction entered an 'engaged' or 'elongating' pool that returned to the 'free' pool on termination. In another, a 'free' population exchanged directly with either an 'engaged' fraction or a 'bound' one (which could only pass to the 'engaged' fraction through the 'free' pool). We believe that discriminating between such models will require the acquisition of more and better data, and the extension of the models to include a more detailed description of the binding and elongation processes, possibly considering the duration of elongation in terms of delay differential equations.

Br-U incorporation

Cells were grown on coverslips in 35-mm dishes for 48 h. For heat shock treatment (Figure 1C), the dishes were surrounded in waxy film, immersed in a water bath for various times (as above), 2.5 mmol/L Br-U added, and the cells grown for 10 min; after fixation (20 min; 20°C)

with 250 mmol/L Hepes, 4% paraformaldehyde, Br-RNA was indirectly immunolabelled using a mouse monoclonal anti-BrdU antibody (1/100 dilution of clone IU-4; Caltag laboratories, Burlingame, CA) and donkey anti-mouse IgG antibodies conjugated with Cy3 (1/200 dilution; Jackson ImmunoResearch Inc, Bar Harbor, ME) and images collected on the confocal microscope (Pombo *et al*. 1999).

Numbers of GFP-pol/cell

The number of molecules of RNA polymerase II in C23 cells growing at 39°C was determined by quantitative immunoblotting by reference to the known number (i.e. 320 000) in a HeLa cell grown at 37°C (Kimura *et al*. 1999). All immunoblotting procedures were conducted at room temperature unless stated otherwise. Cells in a culture dish were lysed by adding a 2 × concentrate of the SDS-containing sample buffer used for electrophoresis, sonicated (10–20 s using level 10 with the microprobe on the Soniprep 150; Sanyo Gallenkamp PLC, Leicester, UK), heated at 98°C for 5 min, and proteins from 10^3 to 5×10^4 cells resolved on 6% SDS-polyacrylamide gels. After blotting on to nitrocellulose (Kimura *et al*. 1999), hypo- and hyper-phosphorylated forms of the largest subunit of RNA polymerase II were detected using a monoclonal antibody (clone 7C2; Besse *et al*. 1995), a donkey anti-mouse IgG conjugated with horseradish peroxidase (Jackson Immunoresearch) and the peroxidase substrate kit (AEC, Vector Laboratories Inc, Burlingame, CA). Digital images were analysed using 'Photoshop' (Adobe Systems Incorporated, San Jose, CA), and the relative amounts of each band determined by interpolation from the intensities (measured in the linear range in the same blot) seen for the corresponding bands given by different dilutions of known numbers of HeLa cells.

Results

FLIP reveals two or more populations

We first repeated the FLIP experiments performed by Kimura *et al*. (2002), and obtained similar results. A field containing two nuclei was

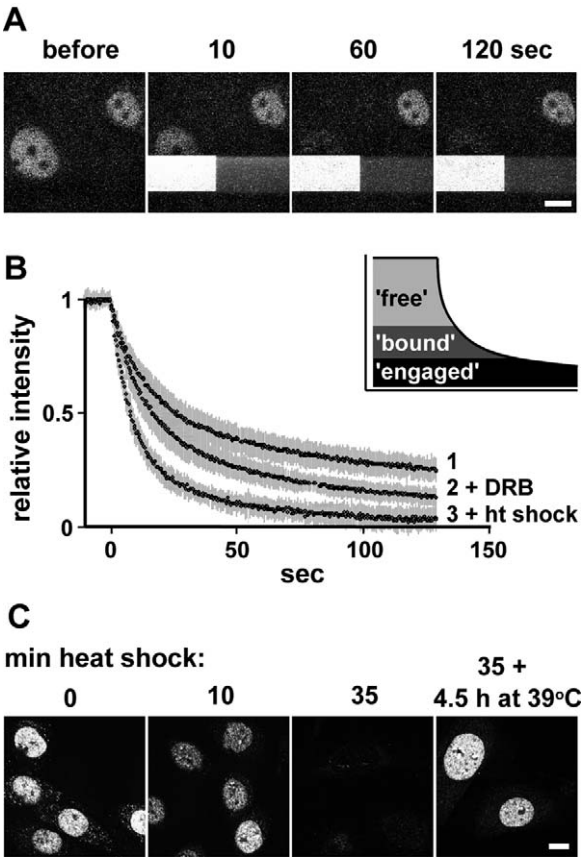

Figure 1. GFP-pol kinetics in C23 cells analyzed using FLIP. (**A**) Example. Images of typical equatorial confocal sections were collected before and after half of the lower nucleus (contained in the white rectangle) was imaged/bleached every 0.43 s for 120 s. The upper nucleus is used as a reference, and the signal to the right of the bleached area is an artifact. Bar: 10 μm. (**B**) Results (relative intensity ± SD; cell number ≥17). Curve 1: untreated cells. Curve 2: cells treated with 100 μmol/L DRB for 25–55 min before and 130 s during bleaching. Curve 3: cells heat-shocked at 45°C for 25–35 min before and 130 s during bleaching. Inset: The kinetics of curve 1 are consistent with there being two (or more) populations that enter the bleaching zone with different kinetics: here, three are shown. One ('free') diffuses rapidly, the second ('bound') is attached temporarily to some nuclear structure but is transcriptionally inactive, while the third ('engaged') dissociates slowly from the template. DRB would release the 'engaged' fraction to increase the size of the 'free' fraction, and heat shock would release both 'bound' and 'engaged' fractions. (**C**) Br-U incorporation falls during heat shock and recovers thereafter. Cells were heat-shocked (45°C) for 0, 10 or 35 min, or heat shocked for 35 min and regrown for 4.5 h ('35 + 4.5 h at 39°C'), and fixed; in each case, 2.5 mmol/L Br-U was added 10 min prior to fixation and the resulting Br-RNA indirectly immunolabelled with Cy3 before equatorial sections were collected using a confocal microscope. Bar: 10 μm.

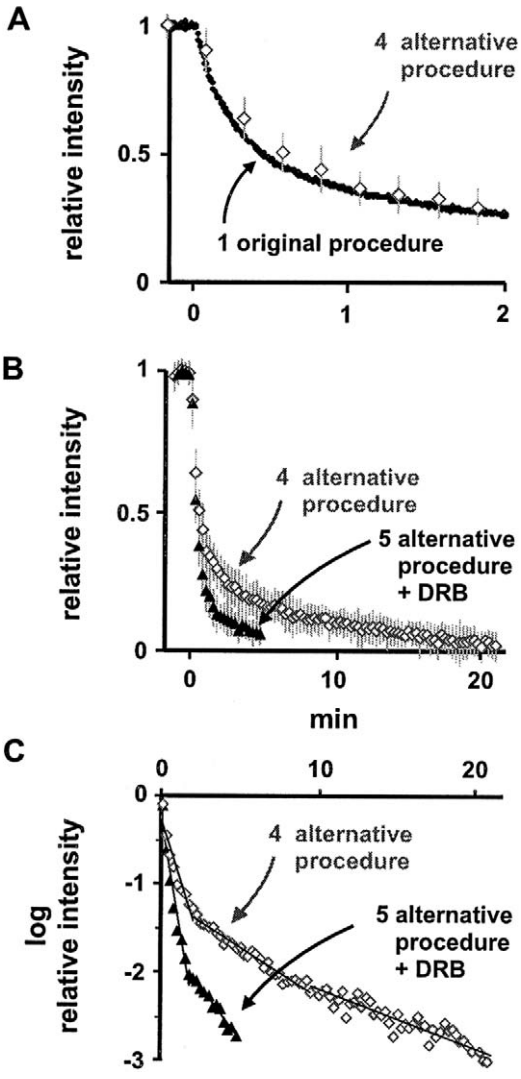

Figure 2. GFP-pol kinetics analysed using an alternative FLIP procedure. The procedure was as in Figure 1A & B except that a 25.7-fold higher laser power was used and imaging/bleaching took place 37.5-fold less frequently (i.e. every 15 s). (**A**) Data obtained during the first 2 min (curve 4). Curve 1 is redrawn from Figure 1B. (**B**) Complete data set for 22 min for untreated cells (curve 4), or cells treated with 100 μmol/L DRB for 25–57 min before and during bleaching/imaging (curve 5). (**C**) Semi-logarithmic plot of data in (**B**). The kinetics underlying curves 4 and 5 are consistent with the existence of at least 3 and 2 populations indicated by the straight lines, respectively.

selected, and raster scanned repeatedly with the laser as images were collected on a confocal microscope (Figure 1A). The laser power was varied during scanning. A low power sufficient for imaging was used for most of each scan, but then the power was increased 25× for bleaching as the laser scanned through a rectangle containing the bottom half of the lower nucleus. Unfortunately, the power fluctuations degrade the image to the right of the rectangle. This process was repeated every ~0.43 s for 120 s until most fluorescence disappeared from the top half of the bottom nucleus. The intensity in the unbleached half of the nucleus was then expressed relative to its original (unbleached) intensity, and the value further corrected for the slight effects of bleaching during imaging (using the reduction in fluorescence seen in the other unbleached nucleus).

We can envisage several different results of such bleaching. If all GFP-pol were freely diffusible, bleaching the bottom half should progressively reduce the (relative) intensity in the top half to zero because unbleached molecules can diffuse into the target area and be bleached; this is the result obtained in control cells expressing GFP (Kimura *et al.* 2002). At the other extreme, all GFP-pol might be immobile, and then the relative intensity remains at unity because immobile molecules in the top half can never enter the bleaching zone; this is the result obtained with fixed cells (Kimura *et al.* 2002). The results lie between these extremes, and are consistent with the existence of two (or more) populations. The larger population would be able to diffuse rapidly into the bleaching zone, while the smaller one leaves the top half of the nucleus more slowly (Figure 1B, curve 1). The first of these two populations would be equivalent to the one labelled 'free' in the inset in Figure 1B, while the second would contain both the 'bound' and 'engaged' populations. [These terms are used operationally. Thus, the 'free' population includes molecules able to translocate rapidly between the two halves of the nucleus. They may bind to – and dissociate rapidly from – chromatin and/or other nuclear structures as they do so, and they may also be part of a large diffusing complex. The 'bound' fraction may include molecules attached temporarily to DNA (perhaps in a pre-initiation complex or 'scaffold'; Yudkovsky *et al.* 2000) or some other nuclear substructure (perhaps in some store).]

Kimura *et al.* (2002) suggest the second population is mainly composed of the engaged fraction (which would include both 'elongating' and 'paused' ternary complexes), and this was supported by an additional experiment using the inhibitor of

transcriptional elongation, DRB (Chodosh *et al.* 1989, Marshall *et al.* 1992, Yamaguchi *et al.* 1998). This drug inhibits P-TEFb kinase and so hyper phosphorylation of the carboxyl-terminal domain (CTD) of RPB1; such hyperphosphorylation is characteristic of the active elongating enzyme. We also repeated these experiments using exposures of <60 min to minimize side effects. As the drug progressively inhibits more and more transcription during the experiment, we monitored the extent of inhibition at different times; the shortest DRB treatment used reduced transcription by polymerase II to ~26% of untreated controls, and the longest to ~8% (Materials and methods). Such treatments with DRB ensured the relative intensity fell further (Figure 1B, curve 2; see also Kimura *et al.* 2002); presumably, any 'bound' and/or 'engaged' polymerases become soluble and so part of the freely-diffusing fraction.

The simplest explanation of all these results is that there are two kinetic fractions, one 'free' and the other DRB-sensitive and 'engaged'. As curve 2 in Figure 1B does not decay to zero (at least in the time analysed), it could be assumed that DRB does not inhibit all transcription by polymerase II (as is the case) and/or some polymerase remains engaged on very long transcription units. However, results are also consistent with other more complicated interpretations, including the possibility that a third DRB-insensitive fraction exists (labelled 'bound' in Figure 1B, inset). We now present data consistent with this more complicated interpretation using a different inhibitor, and an alternative FLIP procedure.

Heat shock destabilizes most polymerase

Growth at 45°C inhibits transcription (Lindquist 1986, Lis & Wu 1993). As photobleaching experiments necessarily extend over a period of time (in our case 25–37 min) during which the heat shock progressively inhibits more and more transcription, we chose a protocol that inhibited transcription to roughly the same extent as DRB so results could be compared. The longest exposures to DRB and 45°C reduce transcription by polymerase II (measured by immunofluorescence after a brief pulse of Br-U) to ~8 and 4% of untreated controls, respectively (Figure 1C; Materials and methods). After the thermal shock before and during FLIP, the relative intensity in the unbleached area fell almost to zero (Figure 1B, curve 3). This provides formal proof that heat shock leads to essentially the complete disengagement of the polymerase from the template so it becomes freely diffusible. The effects of this heat treatment were reversible, as the transcription rate recovers to ~92% of untreated controls after growth at the normal temperature for 4.5 h (Figure 1C; Materials and methods).

DRB and heat shock inhibit RNA polymerase II in different ways; the effects on the relative intensity are also different (Figure 1B, compare curves 2 and 3). This difference suggests there might be at least three kinetic fractions (Figure 1B, inset) – (1) 'free' (diffusible), (2) 'bound' (sensitive to heat shock but not DRB), and (3) 'engaged' (sensitive to both heat shock and DRB). Then, DRB would release only the 'engaged' fraction, while heat shock would release both 'bound' and 'engaged' fractions.

An alternative FLIP procedure reveals multiple kinetic fractions

Kimura *et al.* (2002) did not analyse curves like those in Figure 1 in detail because the interval between successive bleaches was too short to allow equilibration of the mobile fraction throughout the nucleus. Therefore, we lengthened 38-fold the interval between bleaches (i.e. from 0.43 to 15 s) to allow more time for this fraction to equilibrate. We also increased the bleaching power 26-fold to compensate in part for the less-frequent bleaching, and extended the duration of the experiment ten-fold (i.e. to >20 min). This 'alternative' FLIP procedure yields curve 4 in Figure 2A,B. Comparison of the original and 'alternative' procedures (curves 1 and 4 in Figure 2A) shows that the relative intensity given by the 'alternative' initially falls less rapidly; this is expected as the accumulated laser power used for bleaching is less. However, the two curves converge once the mobile GFP-pol is bleached. As essentially all the 'free' fraction is eliminated using the 'alternative' procedure by about 2 min, analysis of the kinetics of the other fraction(s) is facilitated. After bleaching for 20 min, the relative intensity falls to 5% (Figure 2B, curve 4). As

before, pretreatment with DRB ensured the relative intensity fell further and more rapidly (Figure 2B, curve 5); presumably, most 'engaged' polymerases become soluble and so part of the freely-diffusing fraction.

If there were three populations in untreated cells that exchanged with very different kinetics (i.e. 'free', 'bound', and 'engaged'), we might expect to fit a semilogarithmic plot of the data in curve 4 (Figure 2) with three straight lines (as in Figure 2C, curve 4); and – if DRB-treatment eliminated one of these populations – we would expect to fit the data with only two (as in Figure 2C, curve 5). However, fits, though adequate, were imperfect. Nevertheless, results are consistent with the idea that there are (at least) three populations, with one being insensitive to DRB but sensitive to heat shock.

Numbers of molecules in the different fractions

We next correlated the number of molecules of the different forms of the polymerase in the cell with the relative sizes of the different kinetic fractions. Molecular numbers were determined by quantitative immunoblotting (Kimura *et al.* 1999) using an antibody that recognizes the hyper- and hypophosphorylated forms of the C-terminal domain (CTD) of RPB1 (i.e. II_O and II_A; Besse *et al.* 1995). HeLa and the parental CHO-K1 cells contain II_O and II_A, while C23 also contains hypo- and hyperphosphorylated GFP-pol (i.e. GFP-pol II_A and GFP-pol II_O). When C23 is grown at 39°C, it contains little endogenous and temperature-sensitive II_O (Figure 3). We then related the fractions of the different forms to the known numbers of the polymerase in an equivalent number of HeLa cells (Figure 3; Table I).

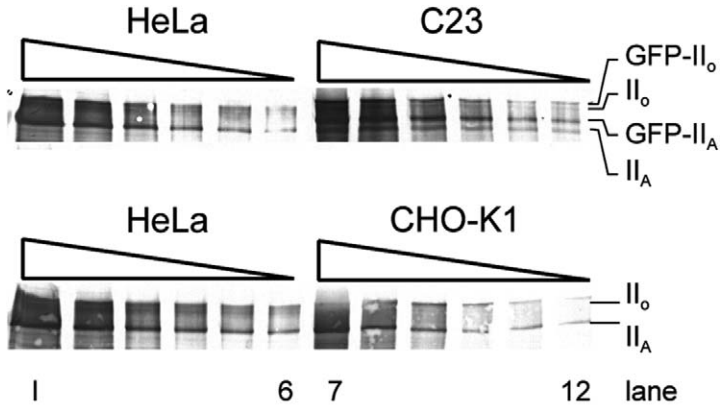

Figure 3. The numbers of molecules of the largest (catalytic) subunit of RNA polymerase II in HeLa, C23, and CHO-K1 cells determined by quantitative immunoblotting. Proteins from 3×10^4 cells (lanes 1, 7), and doubling dilutions (lanes 2–6, 8–12) were resolved on a gel, and the largest subunit detected by immunoblotting using the 7C2 antibody that recognizes both hyper- (II_O) and hypo- (II_A) phosphorylated forms of the CTD.

Table I. The numbers of the different forms of the largest (catalytic) subunit of RNA polymerase II.

	HeLa	**C23**	**CHO-K1**
Total	320 000	480 000	192 000
II_O	170 000[a]	<3000	96 000
GFP-II_O		100 000	
II_A	150 000[a]	130 000	96 000
GFP-II_A		250 000	

Numbers were obtained by quantitative immunoblotting using images like that in Figure 3 (average of 3 experiments), assuming there are 320 000 molecules in a HeLa cell (Kimura *et al.* 1999). HeLa and CHO-K1 were grown at 37°C, while C23 was grown at 39°C. [a]: similar results were obtained by Jackson *et al.* (1998).

Although C23 contains more than twice the total number of molecules as the parental CHO-K1, numbers of the hyperphosphorylated form are similar (compare GFP-II_O in C23 to II_O in CHO-K1 in Table I). This is to be expected: CHO-K1 and C23 have similar sizes and grow at similar rates (Sugaya *et al.* 2000), and it is mainly these forms that are active (Dahmus 1996, Buratowski 2003). Conversely, the (inactive) hypophosphorylated form constitutes ~71% of the total GFP-pol (Table I) compared with the ~75% GFP-pol that constitutes the rapidly exchanging ('free') fraction determined by FRAP (Kimura *et al.* 2002). As expected, then, the 'free' population is hypophosphorylated and inactive.

Discussion

One question arises in any study involving GFP tagging: to what extent does the tagged protein behave like its natural counterpart? The best way of ensuring normal function is to replace the endogenous gene with a hybrid gene encoding the tagged protein, and show that the resulting cells grow normally; this is rarely done in mammalian cells as precise gene replacement is so difficult. An alternative is to utilize a mutant, and demonstrate by genetic complementation that the hybrid gene can restore normal function; this is also rarely done as there are so few mutants. As a result, most studies utilize 'transient' transfections that give populations of variably expressing cells and then it is difficult to prove that the tagged protein functions normally. Here, we used a clonal line expressing the largest (catalytic) subunit of RNA polymerase II (i.e. RPB1) tagged with GFP in addition to the exogenous genes, but this leads to overexpression (Figure 3; Table I). However, we did demonstrate complementation using the appropriate (temperature-sensitive) mutant, so it must be the tagged molecule that keeps this clone alive (Sugaya *et al.* 2000). Moreover, a significant fraction of the GFP-pol (but little of its endogenous temperature-sensitive counterpart) is hyperphosphorylated (Figure 3) and resistant to sarkosyl (Kimura *et al.* 2002), two characteristics of the active enzyme (Dahmus 1996, Buratowski 2003). Even so, the diffusional dynamics of the GFP-tagged protein must differ from the endogenous protein, as it is inevitably 28 kDa larger – the size of the GFP tag. For this and other reasons (Introduction), we concentrate here on changes occurring over the minutes required to complete a transcription cycle (i.e. including initiation, elongation and termination) and not on the changes occurring at shorter times where diffusional kinetics dominate.

Our results confirm and extend those of Kimura *et al.* (2002) and Becker *et al.* (2002). The former expected to find at least three kinetic fractions of GFP-pol: a large pool of enzyme able to diffuse freely, a small fraction incorporated into the pre-initiation complex, and a third that was elongating and so temporarily immobilized on the template. However, data could be fitted assuming there were only two, with ~75% moving rapidly and ~25% being transiently immobile; they concluded parsimoniously that the former was freely diffusing, and the latter was elongating as it could be released with DRB. We now use a different inhibitor – a brief thermal shock (Lindquist 1986, Lis & Wu 1993) – and find that it has a different effect from DRB (even though conditions were chosen so that it inhibits transcription to the same extent). Heat shock leads to almost complete disengagement of the polymerase (Figure 1B, compare curves 1 and 3), formally confirming results obtained less directly (e.g. Gilmour & Lis 1985). [We assume DRB and heat shock decrease the engaged fraction by inhibiting early steps in the transcription cycle, rather than speeding up later steps like elongation and termination.] Data were consistent with there being at least three kinetic fractions – the rapidly-diffusing ('free') one, plus a second sensitive to heat shock but not DRB, and a third sensitive to both heat shock and DRB (Figure 1B). Use of an alternative FLIP procedure also revealed multiple kinetic fractions (Figure 2C).

How do these fractions relate to those known to biochemists? The largest fraction is clearly inactive; it exchanges rapidly (and so cannot be engaged), and FRAP shows that it constitutes ~75% of the total (Kimura *et al.* 2002) which compares with the ~71% found as GFP-II_A by quantitative immunoblotting (Table I). [Most of form II_A is known to be inactive (Dahmus 1996).] Unfortunately, it is difficult to be sure about the other two fractions, which are defined through the action of such unspecific inhibitors, DRB and heat

shock. Nevertheless, one simple interpretation is that one, which is DRB-insensitive but heat-shock sensitive, is bound but not engaged, while the other, which is sensitive to both DRB and heat shock, is elongating.

In order to gain more insight into the transcription cycle and amount of polymerase in the different fractions, data were analysed using models based on the principles of chemical kinetics (Materials and methods). Unfortunately, different models yielded kinetics that, using best-fit values of the model parameters, were consistent with much of our data, and it was difficult to discriminate between them. We believe that suitable models will necessarily have to be more complicated, and so will require more and better data than we have at present to enable us to discriminate between them. These models will probably initially have to include many different populations, so that we can investigate whether some can be eliminated. These populations include those that are exchanging with the cytoplasm, freely-diffusing throughout nuclei, bound transiently but non-productively (e.g. to chromatin or inactive stores; Carrero *et al*. 2003), bound at promoters, contained in pre-initiation complexes, elongating, paused (Law *et al*. 1998), and terminating. They may also have to involve delay differential equations to account for the duration of elongation, possibly with a suitable distribution of delay times to reflect the widely differing lengths of transcription units found in mammalian genomes.

Previous results using fixed cells have demonstrated that nascent transcripts are concentrated in discrete nucleoplasmic sites or 'factories' (Cook 1999). Why, then, are these factories not visible in images like those in Figure 1A, especially when most of the obscuring pool of free polymerases has been removed by photobleaching? There are probably two interrelated reasons. First, a typical factory contains only ~ 8 active polymerase molecules, and it is difficult to image so few GFP molecules in a living cell. Second, the confocal microscope has a resolution (at best) of ~ 700 nm in the z axis. Although individual factories are seen in cryosections of ~ 100 nm, they are too numerous to be resolved in sections of ~ 700 nm. Therefore, imaging factories in living cells awaits technical improvements in sensitivity and resolution.

Acknowledgements

M.H. is a Research Fellow of the Japanese Society for the Promotion of Science. We thank Marc Vigneron (for providing the 7C2 antibody), and The Wellcome Trust (for support).

References

Asturias FJ (2004) RNA polymerase II structure, and organization of the preinitiation complex. *Curr Opinion Struct Biol* **14**: 1–9.

Becker M, Baumann C, John S *et al*. (2002) Dynamic behavior of transcription factors on a natural promoter in living cells. *EMBO Rep* **3**: 1188–1194.

Besse S, Vigneron M, Pichard E, Puvion-Dutilleul F (1995) Synthesis and maturation of viral transcripts in herpes simplex virus type 1 infected HeLa cells: the role of interchromatin granules. *Gene Expr* **4**: 143–161.

Buratowski S (2003) The CTD code. *Nat Struct Biol* **10**: 679–680.

Carrero G, McDonald D, Crawford E, de Vries G, Hendzel MJ (2003) Using FRAP and mathematical modeling to determine the *in vivo* kinetics of nuclear proteins. *Methods* **29**: 14–28.

Chodosh LA, Fire A, Samuels M, Sharp PA (1989) 5,6-Dichloro-1-beta-D-ribofuranosylbenzimidazole inhibits transcription elongation by RNA polymerase II *in vitro*. *J Biol Chem* **264**: 2250–2257.

Cook PR (1999) The organization of replication and transcription. *Science* **284**: 1790–1795.

Dahmus ME (1996) Reversible phosphorylation of the C-terminal domain of RNA polymerase II. *J Biol Chem* **271**: 19009–19012.

Dundr M, Hoffmann-Rohrer U, Hu Q *et al*. (2002) A kinetic framework for a mammalian RNA polymerase in vivo. *Science* **298**: 1623–1626.

Gilmour DS, Lis JT (1985) *In vivo* interactions of RNA polymerase II with genes of *Drosophila melanogaster*. *Mol Cell Biol* **5**: 2009–2018.

Houtsmuller AB, Vermeulen W (2001) Macromolecular dynamics in living cell nuclei revealed by fluorescence redistribution after photobleaching. *Histochem Cell Biol* **115**: 13–21.

Jackson DA, Iborra FJ, Manders EMM, Cook PR (1998) Numbers and organization of RNA polymerases, nascent transcripts and transcription units in HeLa nuclei. *Mol Biol Cell* **9**: 1523–1536.

Kimura H, Tao Y, Roeder RG, Cook PR (1999). Quantitation of RNA polymerase II and its transcription factors in an HeLa cell: little soluble holoenzyme but significant amounts of polymerases attached to the nuclear substructure. *Mol Cell Biol* **19**: 5383–5392.

Kimura H, Sugaya K, Cook PR (2002). The transcription cycle of RNA polymerase II in living cells. *J Cell Biol* **159**: 777–782.

Law A, Hirayoshi K, O'Brien T, Lis JT (1998) Direct cloning of DNA that interacts *in vivo* with a specific protein:

application to RNA polymerase II and sites of pausing in *Drosophila*. *Nucleic Acids Res* **26**: 919–924.

Lee TI, Young RA (2000) Transcription of eukaryotic protein-coding genes. *Annu Rev Genet* **34**: 77–137.

Lindquist S (1986) The heat-shock response. *Annu Rev Biochem* **55**: 1151–1191.

Lippincott-Schwartz J, Snapp E, Kenworthy A (2001) Studying protein dynamics in living cells. *Nat Rev Mol Cell Biol* **2**: 444–456.

Lis J, Wu C (1993) Protein traffic on the heat shock promoter: parking, stalling and trucking along. *Cell* **74**: 1–4.

Marshall NF, Price DH (1992) Control of formation of two distinct classes of RNA polymerase II elongation complexes. *Mol Cell Biol* **12**: 2078–2090.

Phair RD, Misteli T (2001) Kinetic modelling approaches to in vivo imaging. *Nat Rev Mol Cell Biol* **2**: 898–907.

Pombo A, Jackson DA, Hollinshead M, Wang Z, Roeder RG, Cook PR (1999) Regional specialization in human nuclei: visualization of discrete sites of transcription by RNA polymerase III. *EMBO J* **18**: 2241–2253.

Shilatifard A, Conaway RC, Conaway JW (2003) The RNA polymerase II elongation complex. *Annu Rev Biochem* **72**: 693–715.

Sugaya K, Sasanuma S, Nohata J *et al*. (1997) Cloning and sequencing for the largest subunit of Chinese hamster RNA polymerase II gene: identification of a mutation related to abnormal induction of sister chromatid exchanges. *Gene* **194**: 267–272.

Sugaya K, Vigneron M, Cook PR (2000) Mammalian cell lines expressing functional RNA polymerase II tagged with the green fluorescent protein. *J Cell Sci* **113**: 2679–2683.

Tsien RY (1998) The green fluorescent protein. *Annu Rev Biochem* **67**: 509–544.

Tsuji H, Matsudo Y, Tsuji S, Hanaoka F, Hyodo M, Hori T (1990) Isolation of temperature-sensitive CHO-K1 cell mutants exhibiting chromosomal instability and reduced DNA synthesis at nonpermissive temperature. *Somatic Cell Mol Genet* **16**: 461–476.

Woychik NA, Hampsey M (2002) The RNA polymerase II machinery: structure illuminates function. *Cell* **108**: 453–463.

Yamaguchi Y, Wada T, Handa H (1998) Interplay between positive and negative elongation factors: drawing a new view of DRB. *Genes Cells* **3**: 9–15.

Yudkovsky N, Ranish JA, Hahn S (2000). A transcription reinitiation intermediate that is stabilized by activator. *Nature* **408**: 225–229.